Civil Engineering Infrastructures Journal, 52(2): 365 – 377, December 2019
Print ISSN: 2322-2093; Online ISSN: 2423-6691
DOI: 10.22059/ceij.2019.277155.1558

Performance of the Modified Precast Beam to Column Connection Placed on a Concrete Corbel

Bahrami, S.[1] and Madhkhan, M.[2*]

[1] Ph.D., Department of Civil Engineering, Isfahan University of Technology, Isfahan, Iran.
[2] Associate Professor, Department of Civil Engineering, Isfahan University of Technology, Isfahan, Iran.

Received: 02 Mar. 2019; Revised: 14 May 2019; Accepted: 13 Oct. 2019

ABSTRACT: Precast concrete structures in Iran are generally designed as continuous columns with hinged beams, thereby making them simple frames. In this system in site show walls in two directions of buildings guaranteed lateral resisting system. However, in order to obtain a seismic resisting frame, the connection between beam and column should be moment resisting and ductile, allowing the formation of plastic hinges at these connections as well as at the column base. In this paper, experimental tests were conducted for precast concrete elements with modified beam-column connection under cyclic load. The precast connection considered for this study was a semi precast beam with welded longitudinal bars to embedded plate into beam where the beam is connected to corbel with welding embedded plated to plate on the corbel. According to the results, the connection shows suitable performance until drift of 2.75% in terms of stiffness, damping and moment resistance.

Keywords: Concrete Corbel, Energy Dissipation, Precast Beam-Column Connection.

INTRODUCTION

Approximately 90% of the precast building constructed in Iran use hinge beam to column connection. The structural system originally designed in the Western Europe was capable of carrying gravity loads only, and this structural configuration is still common. In recent years engineers are attempting to modify the connection details in order to impart lateral load resistance capacity to the precast buildings.

In major earthquakes, precast concrete structures suffered from catastrophic failure and high levels of damage which was particularly due to lack of ductility and joint failure. This brought joint ductility to the center of attention for precast structures. Due to discontinuity, precast connections are considered disadvantageous for structures that require special attention to design and performance. It is difficult to obtain fully moment resistant beam to column connection in the case of precast buildings, and such attempt would neutralize the advantages of modular construction with precast members.

A semi-rigid connection having 80% the moment resistance capacity of a fully continuous connection shows approximately the same seismic behavior as the rigid system (Sucuoglu, 1995). Consequently, if this can be achieved, then multi-story buildings can be constructed at low cost and at a fast pace, while having desirable mechanical

* Corresponding author E-mail: madhkhan@cc.iut.ac.ir

characteristics.

The PCI (Precast Concrete Institution) conducted a laboratory research in 1987 on 16 precast connections, including 8 moment resisting and 8 simple connections (Dolan and Stanton, 1987). The objective was the optimization of connection properties including energy dissipation, resistance, sustainability, ductility and economic performance. Laboratory models were made by Dolan and Pessiki (1989) at ½ scale, and also a theoretical study was conducted to show the suitability of computer models for analyzing the behavior precast concrete connection.

Laboratory specimens were constructed by Bull and Park (1986) to assess the moment resistant beam-column joint under seismic load in New Zealand. The connection consisted of a placing precast concrete beam with the shape of U at the joint and completing the connection on sight using slabs and concrete. This connection was used in low rise frame structures, and formulation for design of these connections were developed.

French and Amu (1989) tried to place the connection further away from the column face along the beam span. A partially prestressed beam was used along with precast RC (reinforced concrete) column. In this configuration, the details of the reinforcement are complex but they are accurately created in factory conditions for the core of beam-column joint. Due to continuity of reinforcement, the joint has higher integrity, will can prevent premature failure.

Mahmoudi et al. (2016) and Ghassemieh et al. (2017) studied energy absorption in concrete structures under cyclic loading. When midspan connection is used for the beams, the resulting precast system is heavy and transportation of it is difficult because of having large sizes. As a result, cruciform precast members cannot be easily employed for long beams due to difficulty in transportation.

Khaloo and Parastesh (2003) and Parastesh et al. (2014) performed an experimental study on precast concrete connections having a 4/10 scale for various bar percent and stirrup spacing in the beam in order to obtain a moment-resisting joint between precast beam and column at regions having high seismicity. The specimens of cruciform shape were constructed for continuous columns and separate beams. A gap or seat was created at the column with sufficient area for bearing the beam loads at the site. The beams had U-shape cross section near the connection, but the remainder of the cross section had rectangular shape. Overlap of protruding bars from columns and the buried beam creates flexural forces. Based on the test result, the cast-in-place construction can be considered as a viable method for design and construction. The installation in the site requires formwork and temporary vertical support for the beams.

Shariatmadar (2014) studied 3 precast concrete connections on the interior side and a continuous reference connection or MO. Continuous column was used in connection PC3, and discontinuous column was used in PC1 and PC2 connections. For PC1 and PC2, the beam was placed at the column gap. The additional bars for beam and column were placed at the free gap 100 mm above the precast beam, and fresh concrete was cast in the remaining space. In PC3, the beam was placed at the seat, and the pending plates were welded.

Four semi-rigid connections were tested by Elliot et al. (2003) and Gorgun (1996). The beams were supported by a solid section or steel corbel at each column side for shear force resistance. Top beam bars were added at the time of construction through the column. With this system, multi-story buildings can be constructed at a fast speed and with low cost. Bahrami et al. (2017a,b) and Bahrami and Madhkhan (2017)

analytically and experimentally evaluated bahaviour of new proposed precast connections with hidden corbel.

The aim of this paper is an investigation of one type of precast reinforcement connection that is welded connection where the bottom bars of the beam weld to embedded plates and then be welded to plate on the corbel. The objectives of this experiment are to study the behavior of precast joint, and crack pattern, and resistance of the connection to be introduced to industry.

CONNECTION DETAILS

The beam-column connection during construction of the cage in the factory is shown in Figure 1. The concrete columns are prefabricated, continuously cast in the vertical direction with the concrete corbel, which is the seat for the beam. It has sufficient bearing area to accommodate the beam and resist the forces. This design does not need shoring or formwork for the slab/beam. The resulting design is cost efficient and can be quickly constructed. The concrete beam is semi precast, which is placed on the corbel. The plates on top of the corbel are welded to the beam's bottom plates. There are three holes in the columns, which allow passing 2 longitudinal top bars (threaded) from the beams, as shown in Figure 1. The empty space of the connection and two holes in the column is grouted with expansive grout. Subsequently, the connection was completed by the top part of the beam concreting. The semi precast beam, precast column, and assembly and details of this connection are shown in Figures 1 and 2.

In Figure 3, the control specimen configuration (monolithic connection) is shown. ACI 318-11 was used for designing the strong column / weak beam for the 6/10 scale of the real size connection. The beam has a cross section of 250 × 320 mm. The net length of beam span is equal to 1480 mm. The column height is 1440 mm, with a 250 × 250 mm square cross sections. The reinforcement is 8 × T14 (14-mm diameter). Two bars of T16 (diameter of 16 mm) at top and bottom were used. The cover for both column and beam is 20 mm in precast and continuous beams. For the 16-mm diameter bars, the yield stress was 452 MPa; and the ultimate stress was 610 MPa, with a corresponding strain of 22%. For the steel in the corbel, the yield stress was 235 MPa and the ultimate stress was 390 MPa. The concrete had a compressive strength of 30 MPa for both PC and MC specimens. The cast-in-place concrete had a compressive strength of 30 MPa, and the grout had a compressive strength of 43 MPa.

Precast column

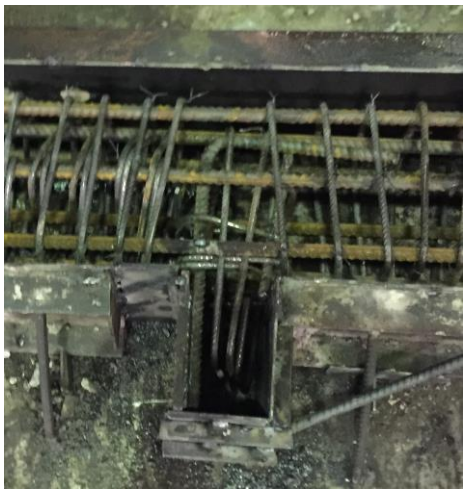

Column and corbel formwork

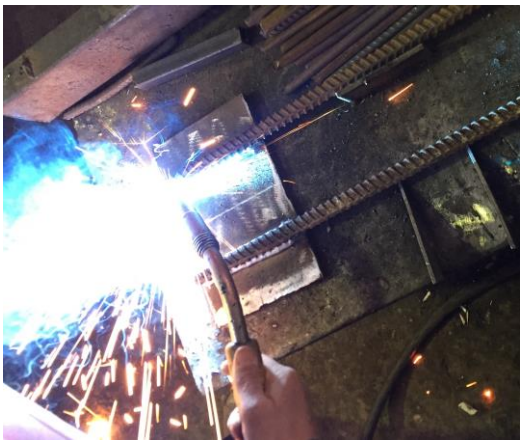

Welding beam bars to plate

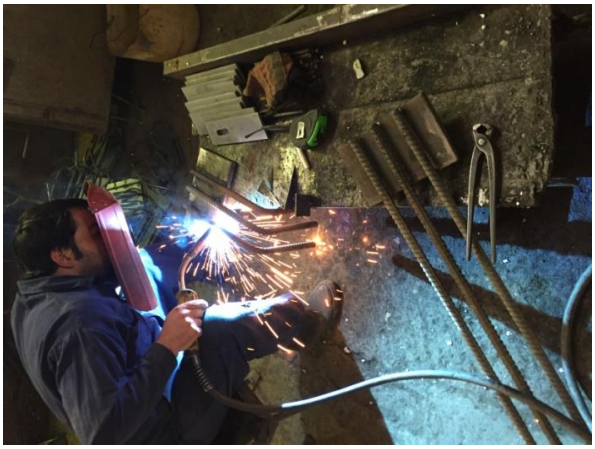

Welding joint bars to plate of corbel

Fig. 1. Steps for precast beam and column construction

Longitudinal bars welded plate into beam

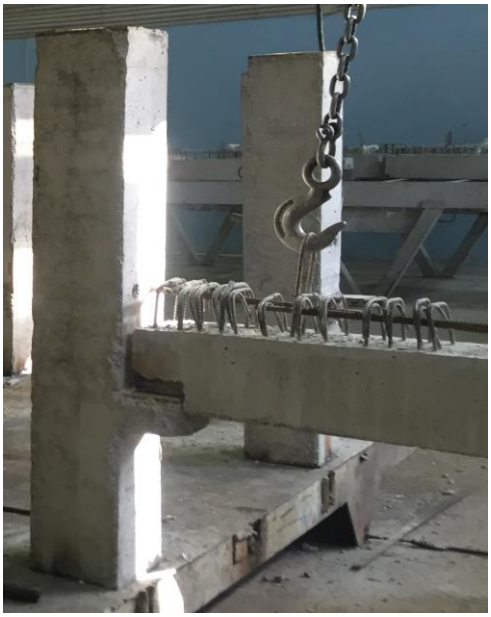

Installing the precast beam on corbel

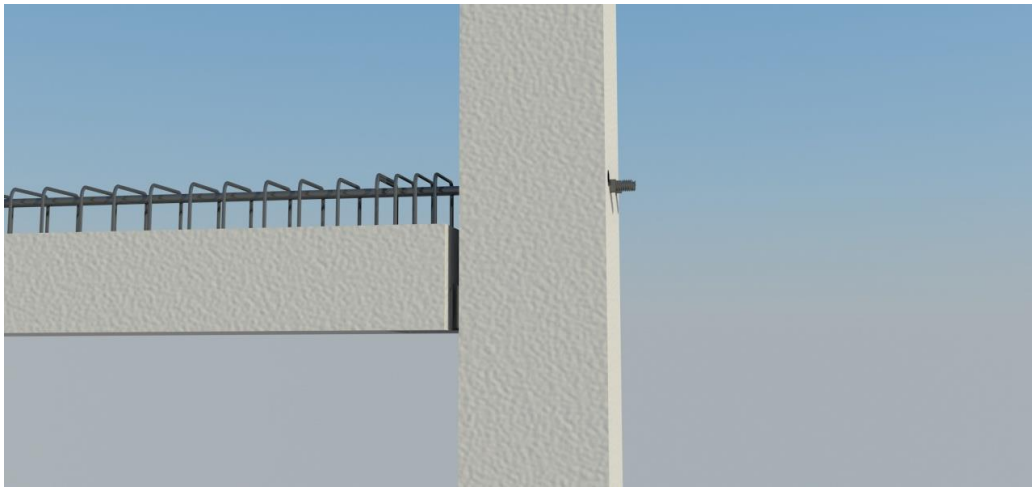

Fig. 1. (Continued), Semi-precast beam with top bars passed through the precast column

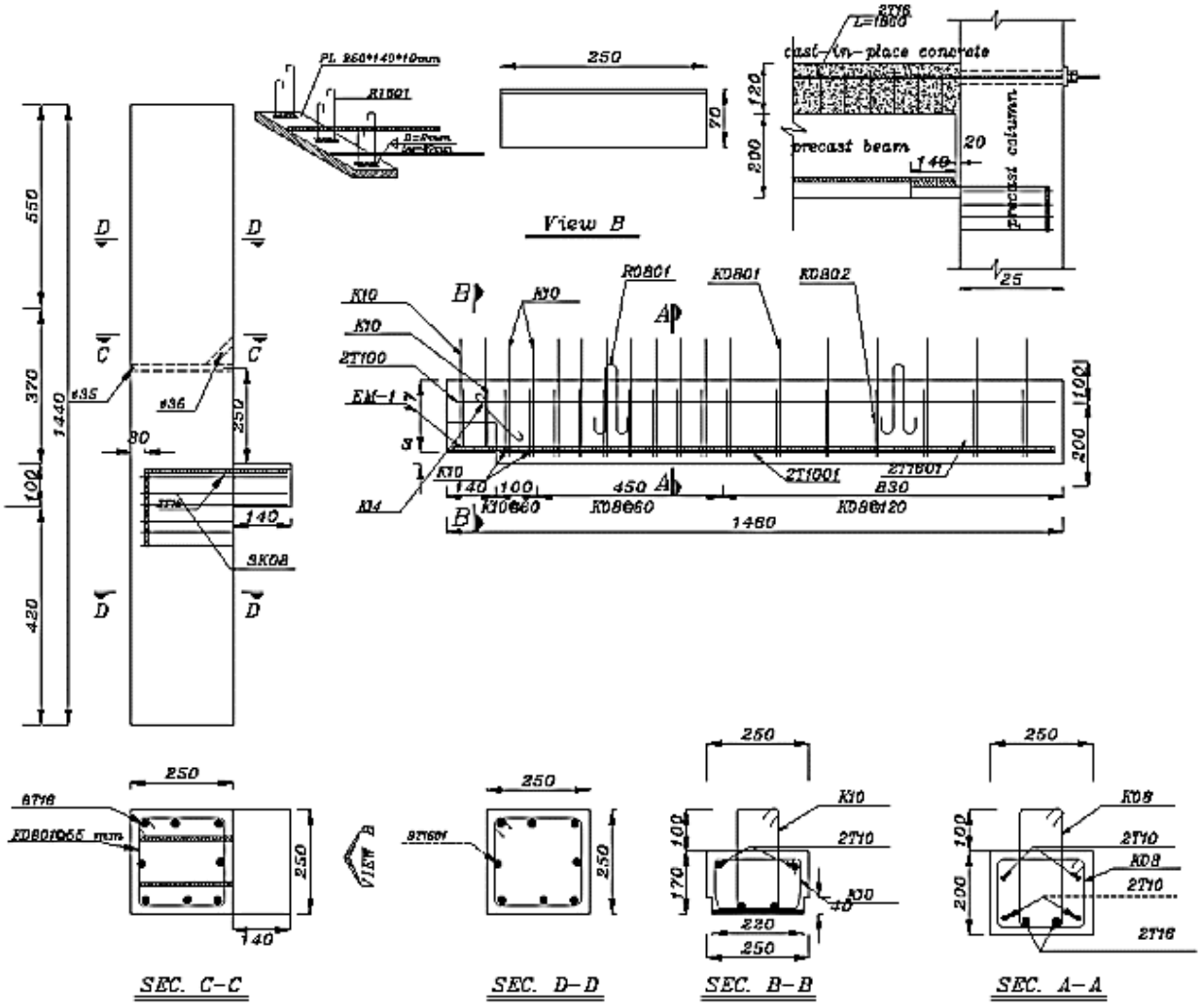

Fig. 2. Details of beam-column connection (specimen PC)

INSTRUMENTATION AND LOADING

Lateral loading was applied to continuous connection MC and precast connection PC based on ACI T1.1-01. The axial force on the precast column was 160 kN, which is 10% of the ultimate axial capacity of the column or 0.1 f'_cA_g, as proposed by Cheok (1997). The column was simply supported at bottom and free at the top. The beam had a roller support at the end. Displacement control tests were conducted with cycling motion based on Figure 4. Three full reverse cycles were used for each defined drift level, which is the column top displacement divided by column length from the LVDT (linear variable displacement transducer) at the top with hinge support center at the bottom. The final drift ratio for tests was 4.5%. A 150-kN hydraulic actuator was used for applying lateral loads at the column top in cyclic fashion. At the end of 3 successive cyclic loadings, new gap openings, cracks and failures were photographed.

Internal and external instruments were installed on the specimens. LVDTs measured lateral top displacement of the column, and it was supported by a steel frame which in turn was connected to the floor. The rebar local strain was measured via electrical resistance strain gauges. The load cell was of electrical resistance type with a capacity of 250 kN

which was calibrated with an accuracy of 0.1%. The horizontal force applied to the top of the column and the vertical load applied to the beam were measured with the load cell. The setup is shown in Figure 5 along with the dimensions and the location of load cells and hydraulic actuators.

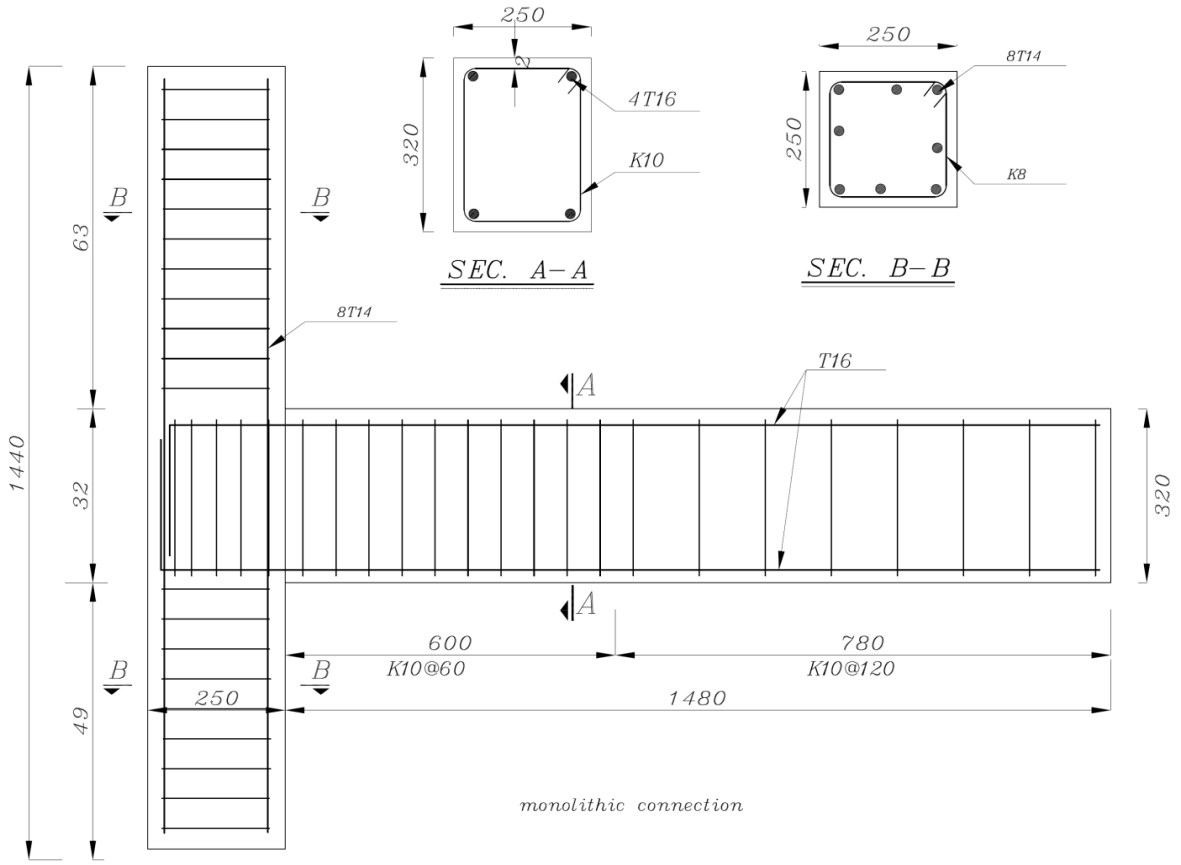

Fig. 3. Continuous connection details for MC specimen

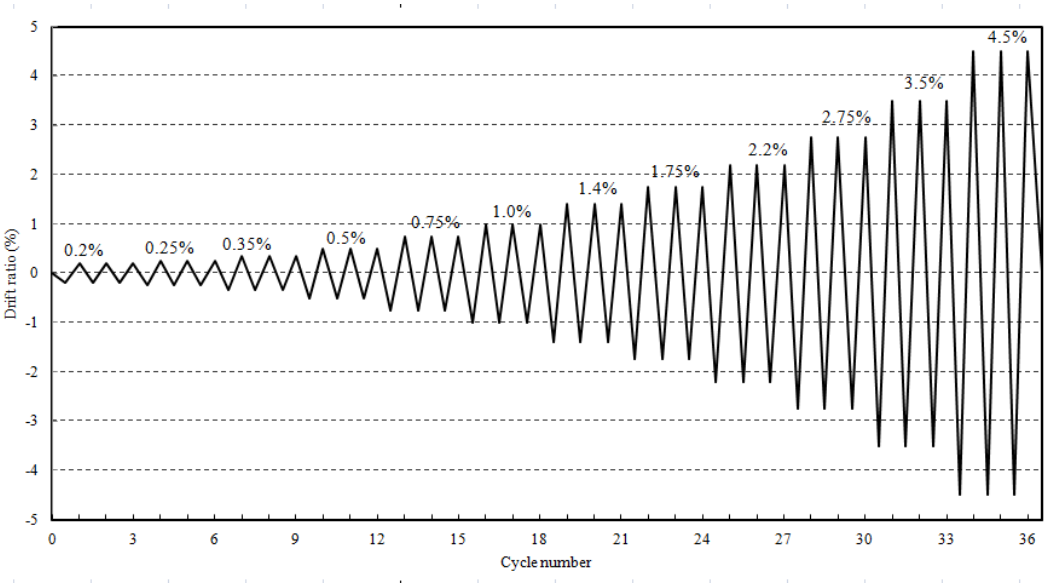

Fig. 4. Time history of cyclic displacement (ACI T1.1-01)

(a) Test set up

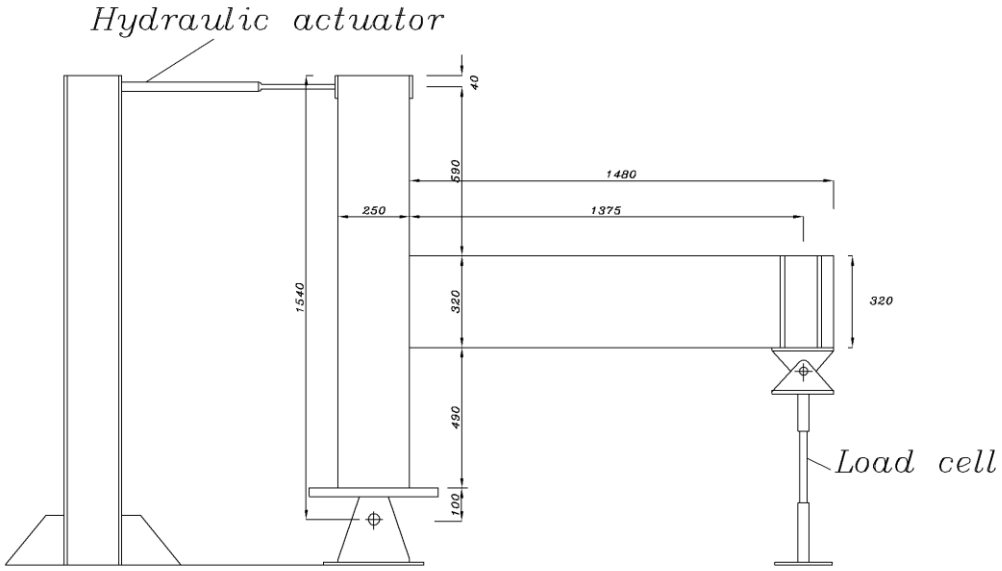

(b) Size and location of hydraulic actuator and load cell

Fig. 5. Test set up and measurement devices

RESULTS

Cyclic loading was continued until failure (Figure 4). The MC and PC seismic behavior was compared with the reference failure mode by comparing ultimate lateral load-bearing capacity as well as dynamic parameters including ductility, damping, stiffness loss and energy dissipation.

Behavior of Specimens

MC Specimen

MC specimen showed elastic response for the first 3 cycles. In the 2nd step, during the first cycle (0.25% drift ratio), bending cracks occurred on the beam 50 mm away from the face of the column. After that flexural and diagonal cracks were distributed along the beam. Yielding of reinforcing bars occurred during the 1st cycle at 1.2% drift ratio. At 1.0% drift level, connection core face suffered from the first diagonal crack. Afterward cracks widened and plastic hinge developed at the first crack in elastic loading. At the 3.5% drift ratio spalling of the beam initiated at the column face. By the time the rest reached its end, there was no strength degradation. The ultimate lateral loads capacity of the MC specimen was 42.7 and 45.5 kN for negative and positive cycles at the end of test respectively. Load versus drift hysteresis response of specimen MC and crack pattern are displayed in Figures 6 and 7 for the drift ratios of +3.5% and -3.5%.

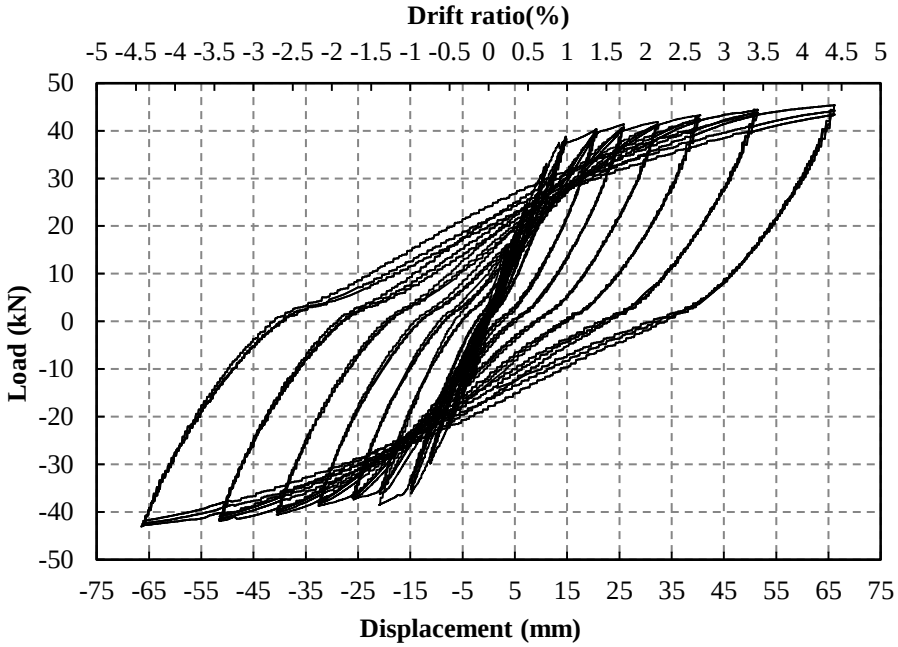

Fig. 6. Lateral load-displacement behavior of MC specimen

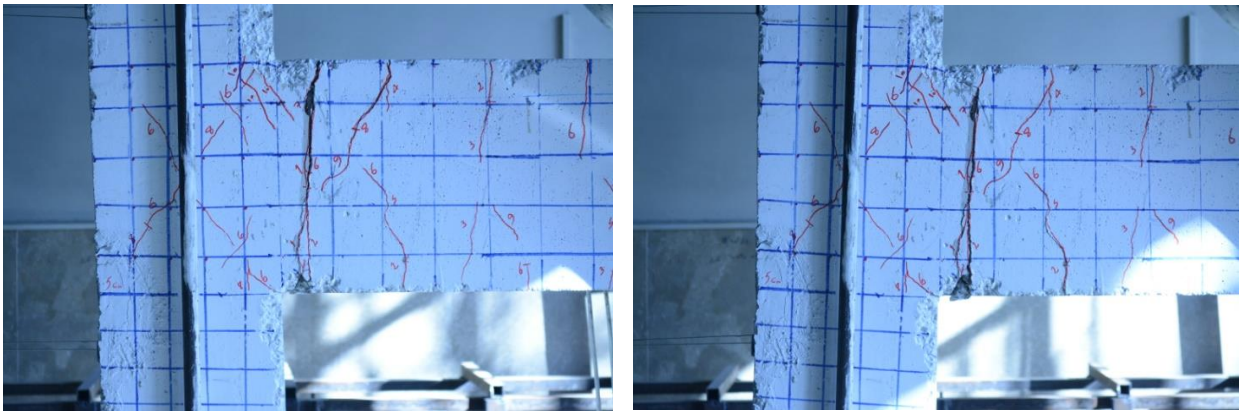

(a) crack pattern at -3.5% drift (b) crack pattern at 3.5% drift

Fig. 7. Crack Pattern of specimen MC at drift: a) +3.5% and b) -3.5%

PC Specimen

Figure 8 shows hysteresis loops of specimen PC by displaying lateral load against column top displacement. Initial cracks appeared at 4 kN negative load at the beam top at the distance 120 mm away from the face of the column, on top of the connection between corbel and beam, which is caused by stress concentration at the point of discontinuity of the interface between corbel and beam. Further increase of the load resulted in extension of bending cracks in the length of the beam. At the bottom, cracks were concentrated at precast beam connection to corbel and a gap opened again at any positive loading. During the 3rd cycle with 1.75% drift, top and bottom cracks joined together. At the load of 25 kN, negative and positive cracks occurred with width of 0.5 mm. At 15th cycle with drift of 0.75%, cracks propagated to the middle of the beam. At cycle number 21 corresponding to drift of 1.3%, top rebars yielded at the load of 32 kN. This was accompanied by widening of the cracks from 0.7 to 1.25 mm which is due to general yielding. The highest backward capacity of the specimen was 41.5 kN at drift of 1.75%, and 42 kN at drift of 2.75% for forward load.

Figure 9 shows that the cracks were mostly concentrated near the top of the beam close to the column and at the beam's bottom near connection to the corbel. At the drift 2.75% bottom longitudinal bars rupture occurred and test terminated. Visual inspection at the end of the test showed the rupture of bottom bars was the main reason for severe damaging in 2.75% drift ratio (Figure 9). Existing cracks in this area widened, while previous cracks did not close during the reverse cycle of the loading. Crushing occurred at the corner of beam near the interface with the column. The hysteresis loops in the loading cycles at 2.75% drift ratio failed which showed significant stiffness degradation and reduced ability to dissipate energy. According to Figure 10, load-drift hysteresis envelopes of two specimens extracted from hysteresis load-displacement curve during cycle number 1 for all drift ratios.

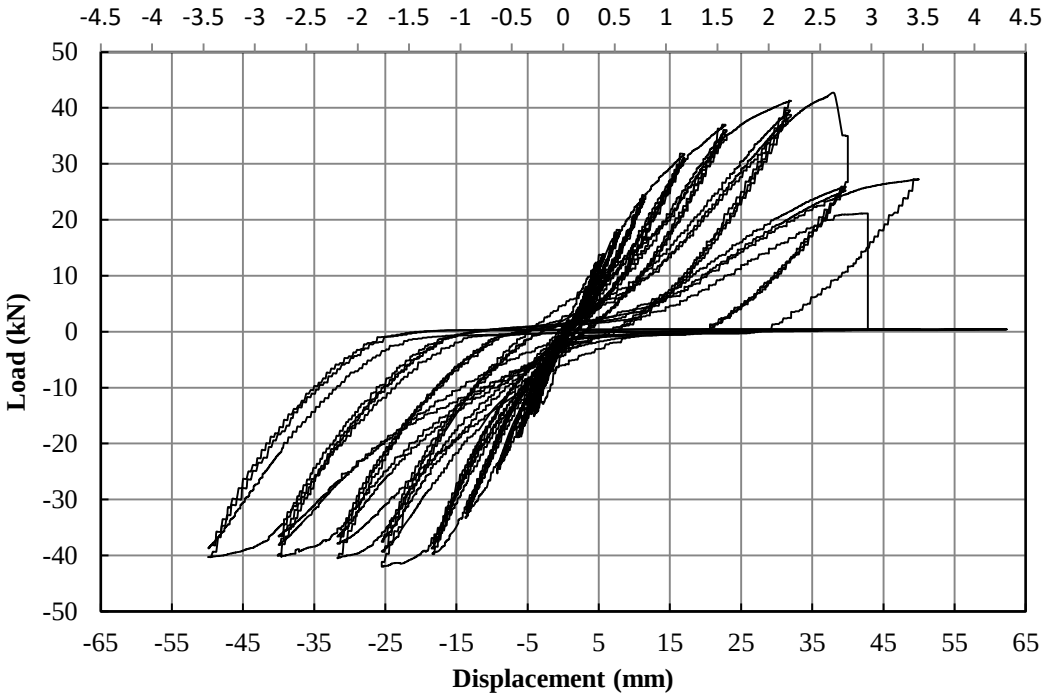

Fig. 8. Lateral load-displacement responses of specimen PC

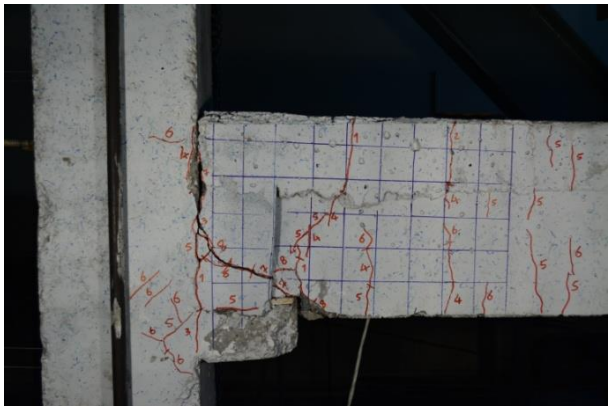

(a) Crack pattern at -3.5% drift ratio

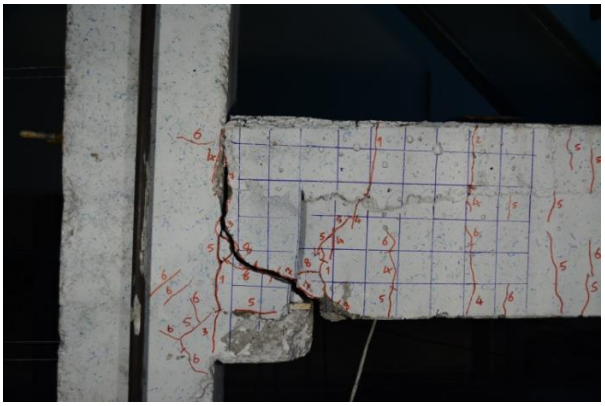

(b) Crack pattern at +3.5% drift ratio

Rupture of beam bars at 2.75% drift ratio

Fig. 9. Crack pattern of specimen PC at drift: a) +3.5% and b) -3.5%

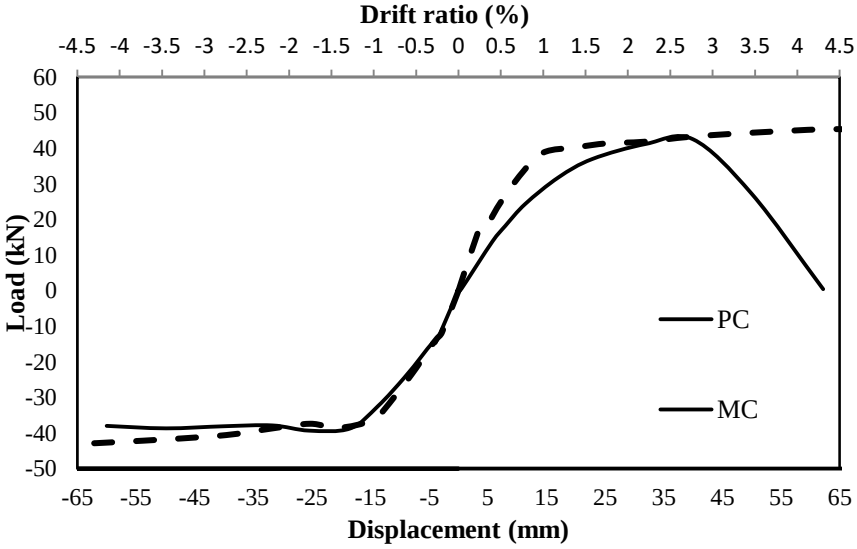

Fig. 10. Envelope hysteresis curves versus drift ratio of specimens

Load and Ductility Capacities

Based on the result, the precast concrete connection was able to reach its ultimate moment strength capacity. The specimen failed at drift 2.75%. Specimen PC exhibited 95% and 96% of maximum capacity in MC specimen for +/- bending moments. Due to strain hardening of the rebars, higher bending moment and load capacity occurred for specimen MC.

Ductility factor indicates the inelastic deformation capacity after the elastic range. In order to preclude brittle failure during earthquake events, higher ductility is desirable. Ductility factors in the precast specimen at positive and negative loading and the corresponding ultimate load capacities are given in Table 1 for specimen MC and the result is compared with other cases. In Table 1, μ: is ductility factor, δ_y: is yield displacement, δ_u: is ultimate displacement and P_{max} : is the maximum load capacity in each specimen. Calculation of ductility was conducted based on that suppose and methods proposed by Park.

Degradation of Stiffness

Specimen stiffness was evaluated via the load-displacement curve and the hysteresis response. This parameter is important in determining the member's behavior during seismic loading. The curve slope is a measure of the specimen stiffness. This would show that for MC the stiffness decreases progressively through the wider cycles down to about ¼ the original one at 4.5% drift, while for PC it decreases rapidly down to very low values (around zero) due to the large gaps left in the connection after any loading cycle.

Table 1. Load capacity, yielding and ultimate displacement and ductility factor of specimens

Direction of load	**Positive loading**				**Negative loading**			
Specimen	P_{max}, kN	δ_y, mm	δ_u, mm	μ	P_{max}, kN	δ_y, mm	δ_u, mm	μ
MC	45.4	13.3	> 66.6	> 5.00	43.1	15	> 66.6	> 4.44
PC	42	20	41	2.05	41.5	18	50	2.78

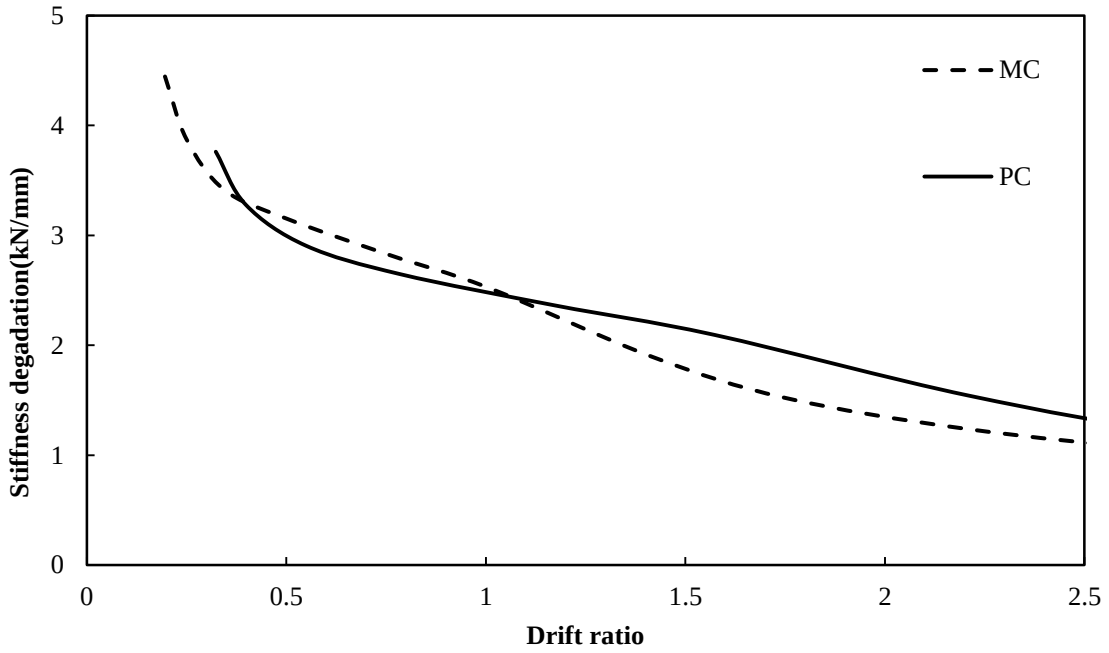

Fig. 11. Secant stiffness degradation versus drift ratio for the specimens

Here, we considered the maximum load and drift point corresponding to negative and positive directions of each loading cycle, and the straight line was drawn to calculate the peak-to-peak or secant stiffness. Changes in secant stiffness at the specimens is shown in Figure 11. PC specimen showed a higher stiffness than the monolithic before 0.9% drift ratio. PC specimen lost 75-80% of the initial stiffness at the end of the test with a drift of 2.75%. The severe stiffness degradation in the PC specimen was more pronounced due to bond deterioration of top bars at column holes and gap opening at the beam and corbel face.

Equivalent Viscous Damping

Equivalent viscous damping ratio is a dimensionless number for measuring the ability of members to dissipate energy. The equivalent viscous damping ratio ξ vs. drift ratio was plotted in Figure 12 to compare energy dissipation properties of the specimens. ξ: is defined in Eq. (1) which is based on the viscous damping definition of Chopra. In this relation, A_p: is dissipated energy and A_e: is elastic peak to peak strain energy.

$$\xi(\%) = \frac{1}{2\pi}\frac{A_p}{A_e} \times 100 \qquad (1)$$

Figure 12 shows that viscous damping is positively correlated with drift ratio for all specimens. At 2.5% drift ratio damping ratio for specimens MC and PC was equal to 9%.

CONCLUSIONS

Precast beam connection to continuous column with a corbel was studied experimentally in this paper to assess the performance of the moment-resistant joint. The beam and column were constructed as precast concrete members. After connecting the beam to column corbel by welding, the gap between the precast beam and top of the beam were monolithically constructed by using non-shrinkage grout and cast-in-place concrete respectively. Specimen PC had good load-carrying characteristics which makes it a good rival for ordinary continuous specimens (MC). It should be noted though, that the failure mode was not favorable.

ACKNOWLEDGMENT

The authors would like to acknowledge the contribution of Deesman Precast Concrete Company in Isfahan, Iran for construction of specimens.

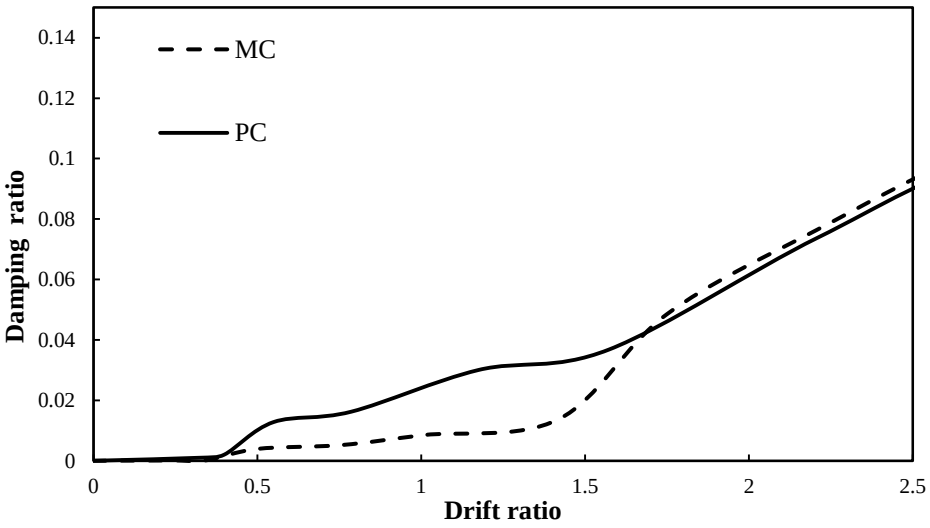

Fig. 12. Plot of damping ratio against drift ratio

REFERENCES

ACI Committee. (2014). *Building code requirements for reinforced concrete and commentary*, ACI 318-14/ACI 318R-14, American Concrete Institute, Detroit.

ACI T1.1-01. (2011). *Acceptance criteria for moment frames based on structural testing*, Reported by ACI Innovation Task Group 1 and Collaborators.

Bahrami, S., Madhkhan, M. and Nazemi, N. (2017a). "Behavior of two new moment resisting precast beam to column connections subjected to lateral loading", *Journal of Engineering and Applied Sciences*, (in press).

Bahrami, S., Madhkhan. M. and Shirmohammadi, F. (2017b). "Behavior of two new moment resisting precast beam to column connections subjected to lateral loading", *Engineering Structures*, 132, 808-821.

Bahrami, S. and Madhkhan, M. (2017). "Experimental performance of a new precast beam to column connection using hidden corbel", *Asian Journal of Civil Engineering*, 18, 791-806.

Bull, D. and Park, R. (1986). "Seismic resistance of frames incorporating precast prestressed concrete beam shells", *PCI Journal*, 31, 54-93.

Cheok, G. (1997). "Hybrid reinforced precast frame for seismic regions", *PCI Journal*, 42, 20-32.

Dolan, W., Pessiki, S. (1989). "Model testing of precast concrete connections", *PCI Journal*, 34, 84-103.

Dolan, CW. and Stanton, JF. (1987). "Moment resistant connections and simple connections", *PCI Journal*, 32, 62-74.

Elliot, K., Davies, G. and Ferreira, M. (2003). "Can precast concrete structures be designed as semi-rigid frames? Part 1: The experimental evidence", *The Structural Engineer*, 81, 14-27.

French, C. and Amu, O. (1989). "Connections between precast elements-failure outside connection region", *Journal of Structural Engineering*, 115, 316-40.

Ghassemieh, M., Saneeinia, Z. and Baei, M. (2017), "Concrete filled tubular bracing subjected to cyclic loading", *Civil Engineering Infrastructures Journal (CEIJ)*, 50(1), 165-177.

Görgün, H. (1996). "Semi-rigid behavior of connections in precast concrete structures", Doctoral Dissertation, University of Nottingham.

Khaloo, A. and Parastesh, H. (2003). "Cyclic loading response of simple moment-resisting precast concrete beam-column connection", *ACI Structural Journal*, 100(4), 440-445.

Mahmoudi, M., Mortazavi, S.M. and Ajdari, S. (2016). "The effect of spandrel beam's specification on response modification factor of concrete coupled shear walls", *Civil Engineering Infrastructures Journal (CEIJ)*, 59(1), 33-43.

Parastesh, H., Hajirasouliha, I. and Ramezani, R. (2014). "A new ductile moment-resisting connection for precast concrete frames in seismic regions: An experimental investigation", *Engineering Structures*, 70, 44-57.

Shariatmadar, H. (2014). "An investigation of seismic response of precast concrete beam to column connections: Experimental study", *Asian Journal of Civil Engineering-Building and Housing*, 15, 49-67.

Sucuoglu, H. (1995). "Effect of connection rigidity on seismic response of precast concrete frames", *PCI Journal*, 40, 94-103.